

**Stem Cell Reports, Volume 16**

**Supplemental Information**

**Erythroid precursors and progenitors suppress adaptive immunity and  
get invaded by SARS-CoV-2**

**Shima Shahbaz, Lai Xu, Mohammed Osman, Wendy Sligl, Justin Shields, Michael Joyce, D.  
Lorne Tyrrell, Olaide Oyegbami, and Shokrollah Elahi**

## **Experimental Procedures**

**Antibodies and flow cytometry.** Fluorophore or biotin-conjugated antibodies with specificity to human cell surface antigens and cytokines were purchased mainly from BD Biosciences or Thermo Fisher Scientific and in some occasions from other suppliers. Specifically, the following antibodies were used: anti-CD3 (HIT3a), anti-CD4 (RPA-T4), anti-CD8 (RPA-T8), anti-CD45 (H-130 or 2D1), anti-VISTA (B7H5DS8), anti-107a (H4A3), anti-PD-L1 (MIH1), anti-CD147 (8D12), anti-CD16 (B73.1), anti-CD56 (B159), anti-CD15 (HI98), anti-CD14 (M5E2), anti-IL-2 (MQ1-17H12), anti-TNF- $\alpha$  (MAB11), anti-IFN- $\gamma$  (4S.B3), anti-CD71 (MA712), anti-CD235A (HIR2) and arginase I (IC5868N/R&D). ROS (Sigma) and arginase II (abcam) staining were performed per the manufacturer's protocols and our previous reports (Dunsmore et al., 2018a; Elahi et al., 2013; Namdar et al., 2019). In addition, anti-ACE2 (535919) from R&D, and anti-TMPRSS2 (EPR3862) from abcam were used for staining. The SARS-CoV-19 spike receptor binding domain protein was purchased from VIROGEN (Cat#00224-V), conjugated with dye using Fluorescent protein labeling kit according to the manufacturing protocol (Thermo Fisher Scientific) for related studies. Besides, Live/dead fixable dead cell stains (ThermoFisher) were used to exclude dead cells in flow cytometry. Paraformaldehyde fixed cells were acquired by flow cytometry using a LSRFORTESSA flow cytometer (BD) and analyzed with FlowJo software.

**Co-culture and stimulation.** For co-culture, a fixed number ( $1 \times 10^6$ ) of PBMCs were seeded into 96 well round bottom plates individually or together with autologous CECs at 1:1 ratio, Brefeldin A (10  $\mu$ g/ml) was added at the same time. In other experiments, PBMCs were stimulated with SARS-CoV-2 peptide pools of S and N (2  $\mu$ g/ml) (Miltenyi Biotec) in the presence or absence of CECs. Similar approach was used for proliferation assay, in brief,

PBMCs were labelled with CFSE and stimulated with peptide pools in the presence or absence of CECs (1:1 ratio) for 3 days.

**Virus infection and quantification.** SARS-CoV-2 stocks were pre-incubated with ViroMag transduction reagent (OZ Biosciences). To remove background virus, cells were washed and pelleted five times with 15 ml of media, a sample of the last wash was taken to measure remaining background viral RNA ( $\sim 10^5$  viral copy). In some experiments, target cells were pre-treated with dexamethasone (2  $\mu\text{g/ml}$ ) overnight prior to the infection. Following a 24-hour incubation at 37°C, a sample of the culture supernatant was taken to measure extracellular virus production. RNA was extracted using QIAamp Viral RNA mini kit (Qiagen). To measure intracellular RNA, cells were first washed and pelleted five times with 15 ml of PBS then lysed with QIAzol reagent (Qiagen), RNA was extracted according to manufactures directions. Reverse transcription was carried out using Superscript IV Vilo master mix (Invitrogen). Quantitative PCR was carried out using primers and probe designed by the United States center for disease control and prevention: for the N gene (N2 primers) of SARS-CoV-2 and RNase P housekeeping gene (IDT cat#10006606). A standard curve was generated using dilutions of positive control standards from CDC (IDT cat # 10006625).

### **Western blot analyses**

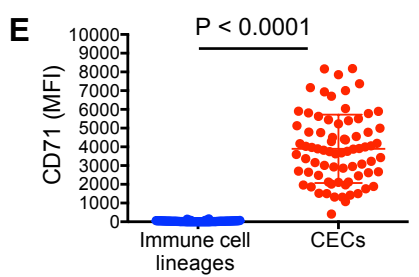
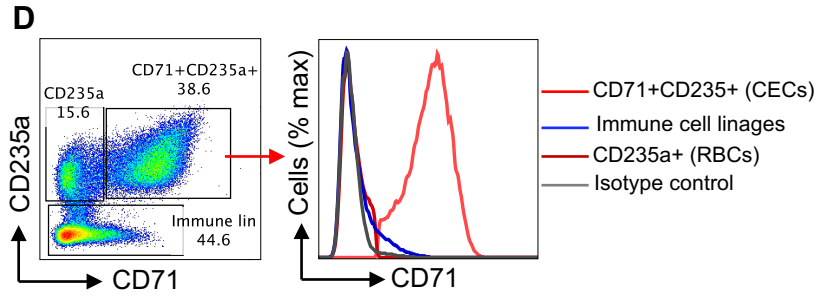
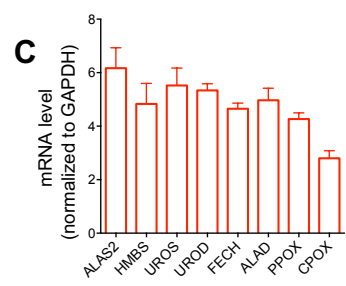
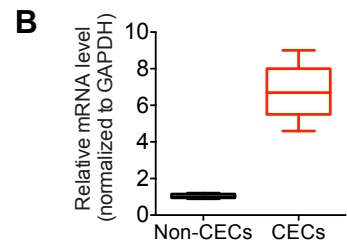
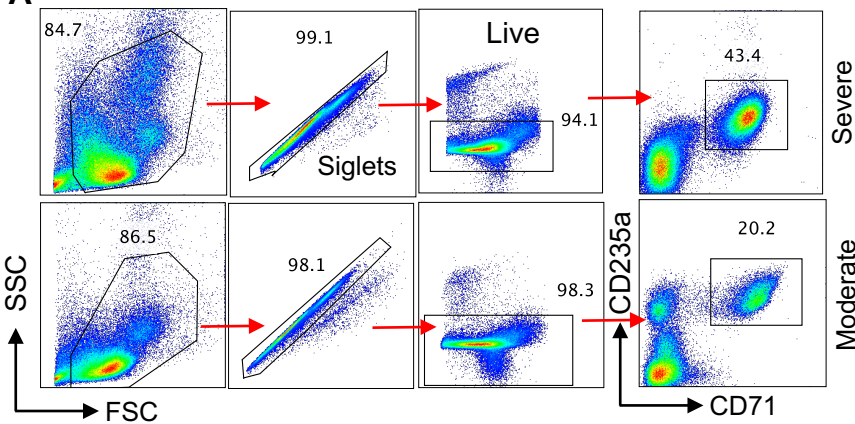
Cells and tissues were lysed in lysis buffer supplemented with a protease inhibitor cocktail (Sigma-Aldrich) and protein concentration was determined using a BCA assay kit (Thermo Fisher Scientific). Protein samples were separated by electrophoresis on either 7%, 17% or 4-15% gradient polyacrylamide gels and then transferred to PVDF membranes. The membranes were blocked with 5% milk and incubated with anti-ACE2 (Abcam, ab15348), anti-TMPRSS2 (Abcam, ab242384) and anti- $\beta$ -actin (Sigma, A2228) antibodies using dilutions 1:1,000. HT29

(human colorectal adenocarcinoma grade II) whole cell lysate was used as a positive control for TMPRSS2 (Abcam, ab3952). Full length predicated at 54 kDa and the cleavage fragment at 25. Next, membranes were incubated with the appropriate HRP-conjugated secondary antibodies and developed using an enhanced chemiluminescence detection kit (Thermo Fisher Scientific).

### **Gene expression analysis**

RNA isolation and qPCR were conducted according to our published data. The resulting cDNA (5 ng/ $\mu$ l) was used as a template for TaqMan qPCR (Applied Biosystems). Each sample was run in duplicates on CFX96 Touch<sup>TM</sup> Real-Time PCR Detection System (BioRad). Beta actin was used as a reference gene, and the gene expression of the targeted genes was calculated by the  $2^{-\Delta\Delta C_t}$  method. SYBR Green Assay primers (human CPOX, PPOX, ALAD, FETCH, UROD, UROS, HMBS, ALAS2 and house-keeping gene) were purchased from BIO-RAD.

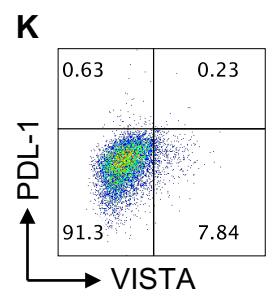
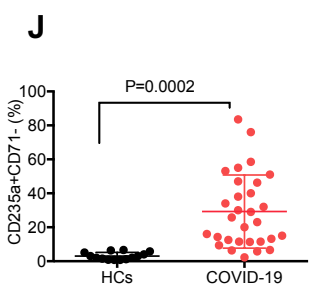
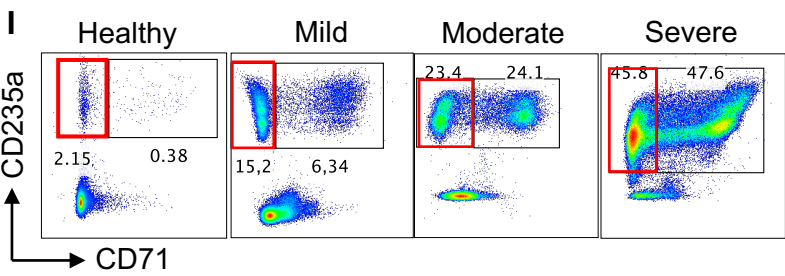
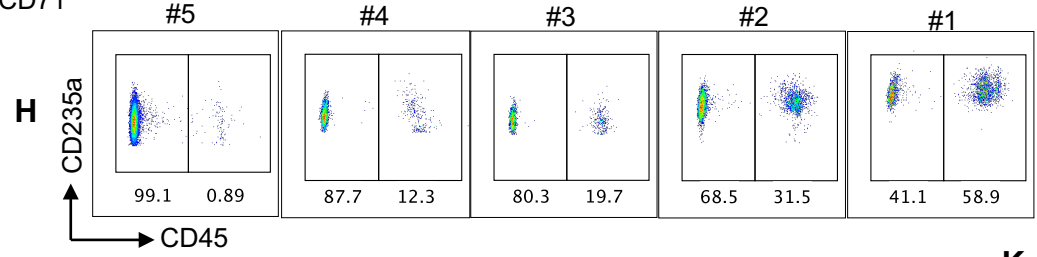
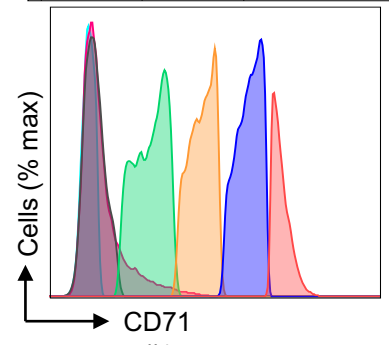
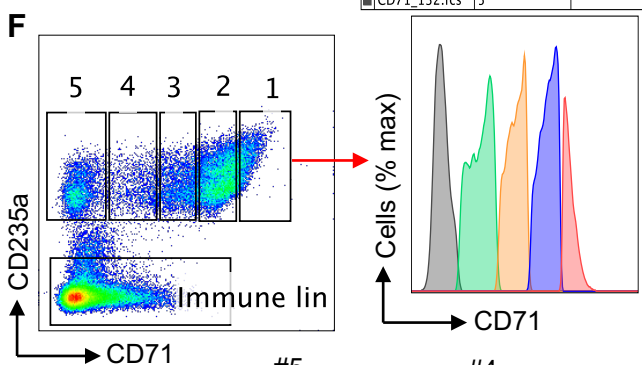
### A S. Fig. 1



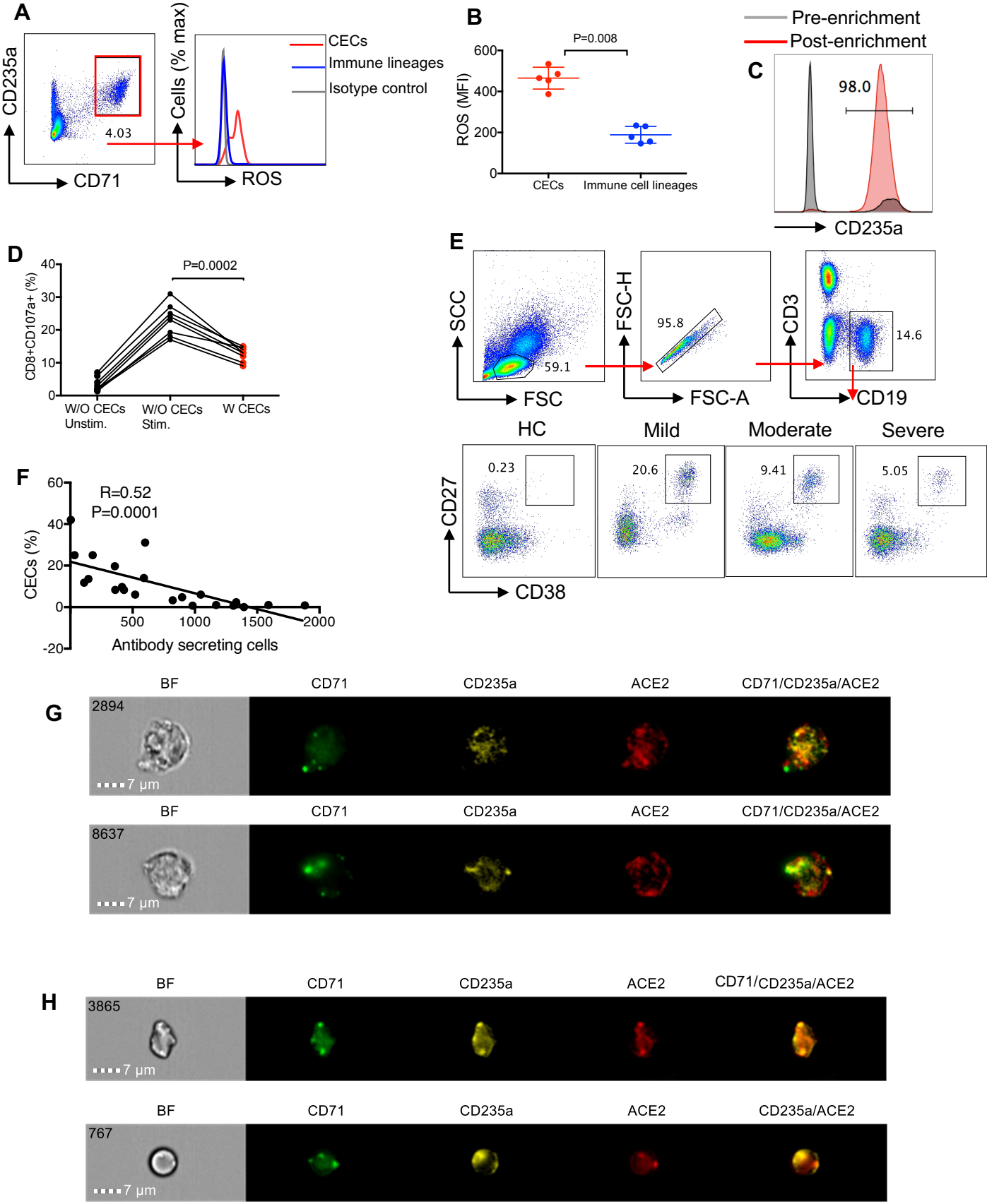
| Sample Name  | Subset Name | Geometric Mean : Comp-R670-A |
|--------------|-------------|------------------------------|
| CD71_132.fcs | 1           | 12831                        |
| CD71_132.fcs | 2           | 4743                         |
| CD71_132.fcs | 3           | 1175                         |
| CD71_132.fcs | 4           | 284                          |
| CD71_132.fcs | 5           | 26.2                         |

### G

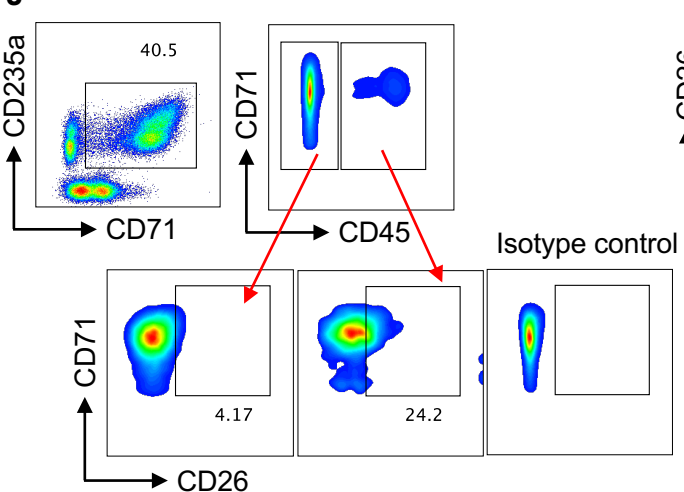
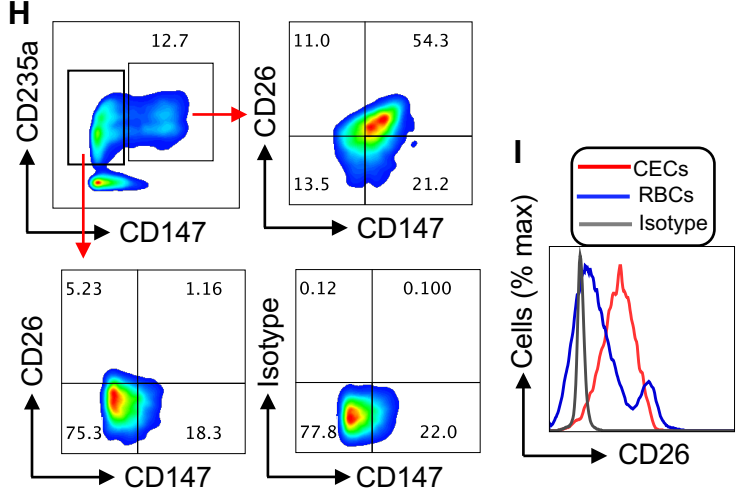
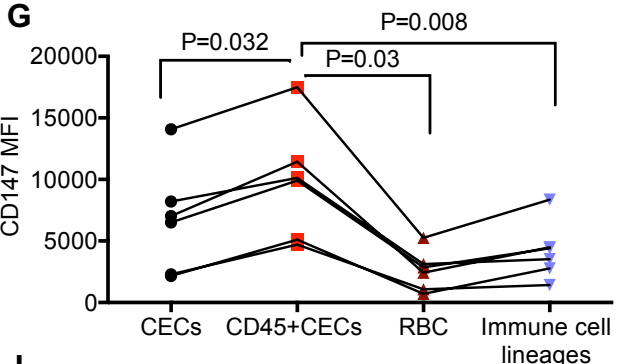
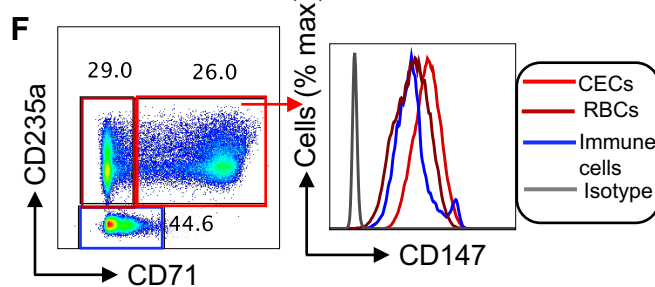
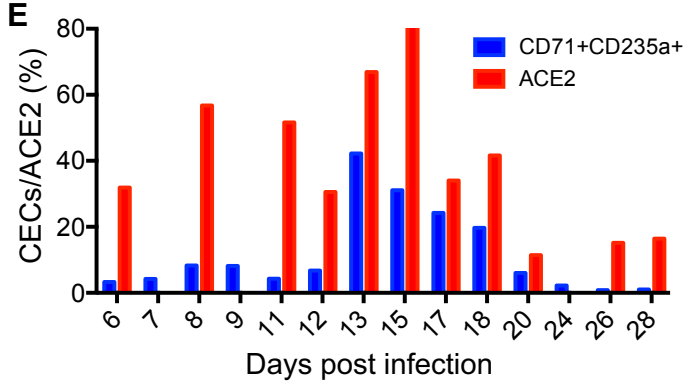
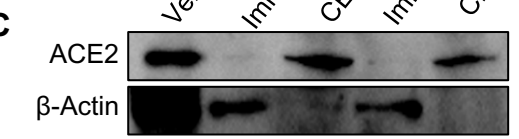
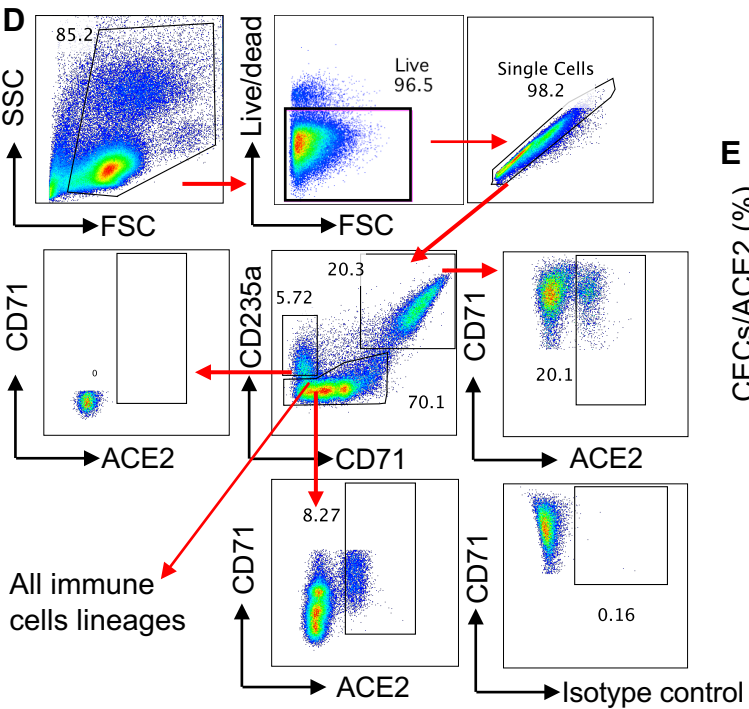
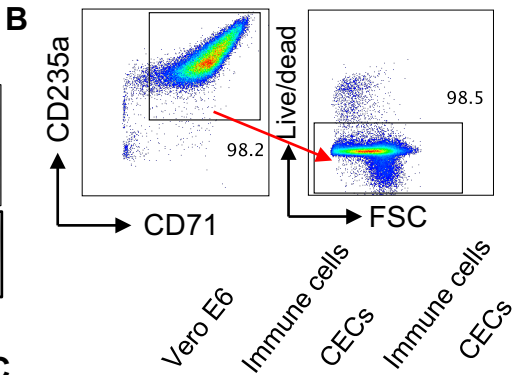
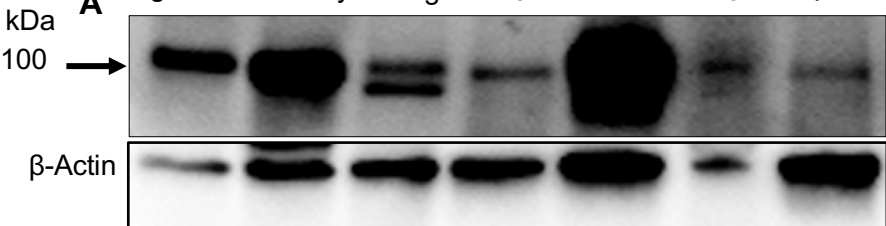
| Sample Name  | Subset Name     | Geometric Mean : Comp-R670-A |
|--------------|-----------------|------------------------------|
| CD71_132.fcs | 1               | 12831                        |
| CD71_132.fcs | 2               | 4743                         |
| CD71_132.fcs | 3               | 1175                         |
| CD71_132.fcs | 4               | 284                          |
| CD71_132.fcs | 5               | 26.2                         |
| CD71_132.fcs | Immune lin      | 52.2                         |
| CD71_140.fcs | Isotype control | 6.53                         |



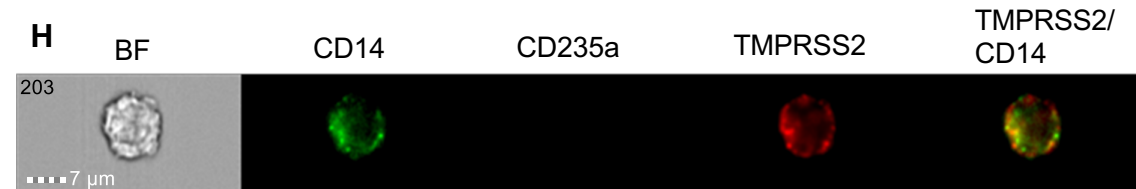
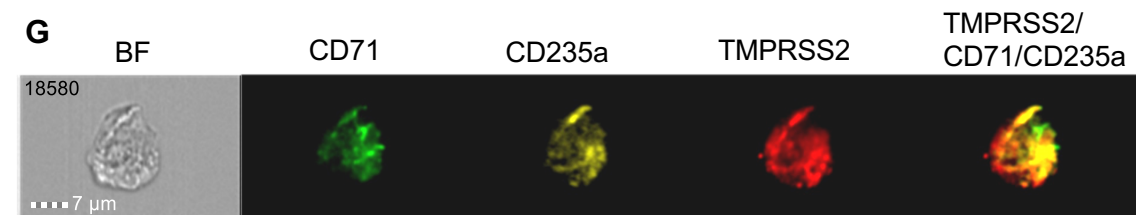
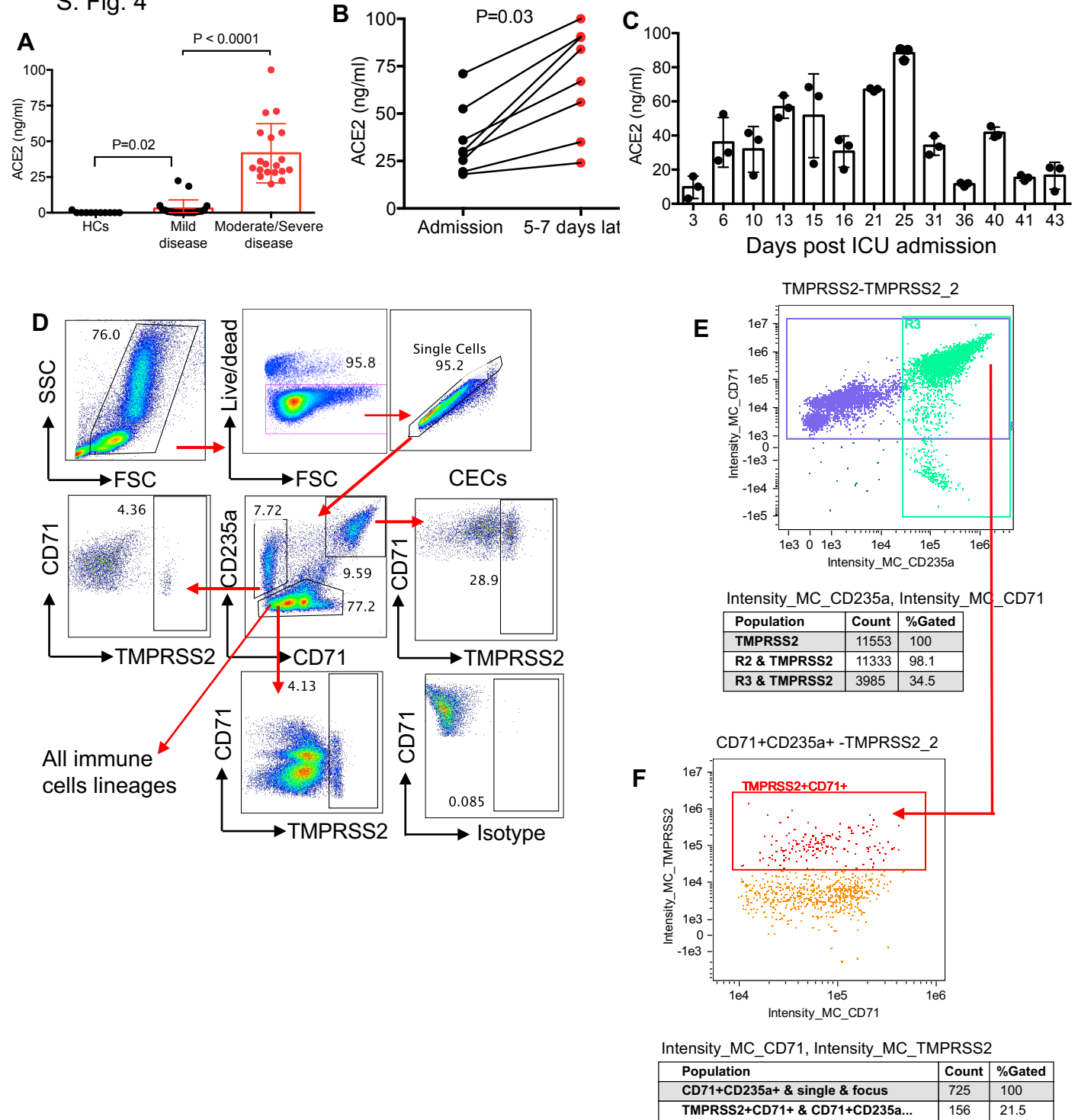
S. Fig. 2



S. Fig. 3 Prostate gland Kidney Lungs Brain Gut Liver Spleen

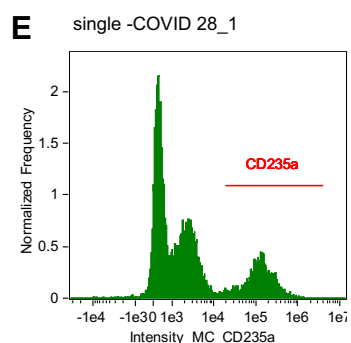
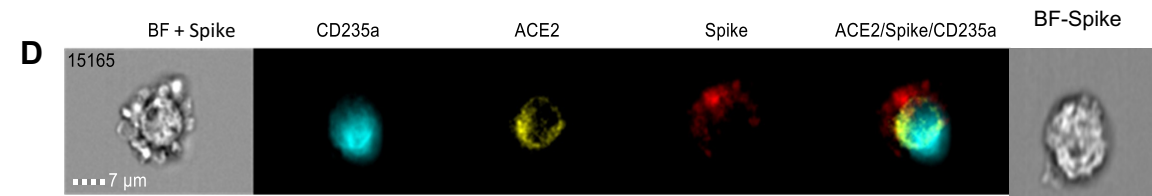
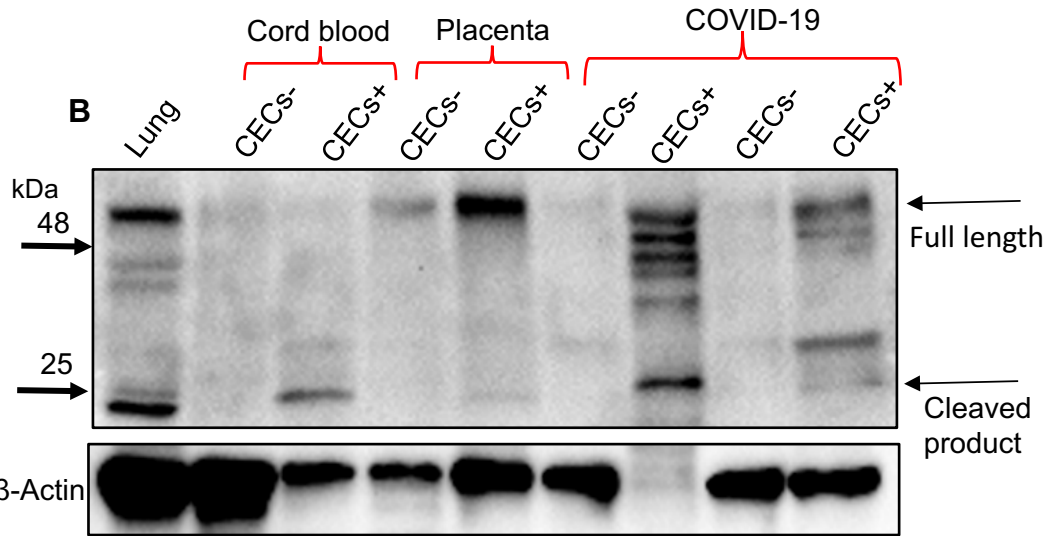
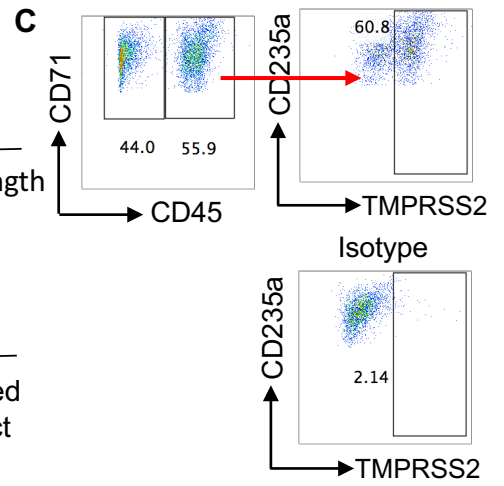
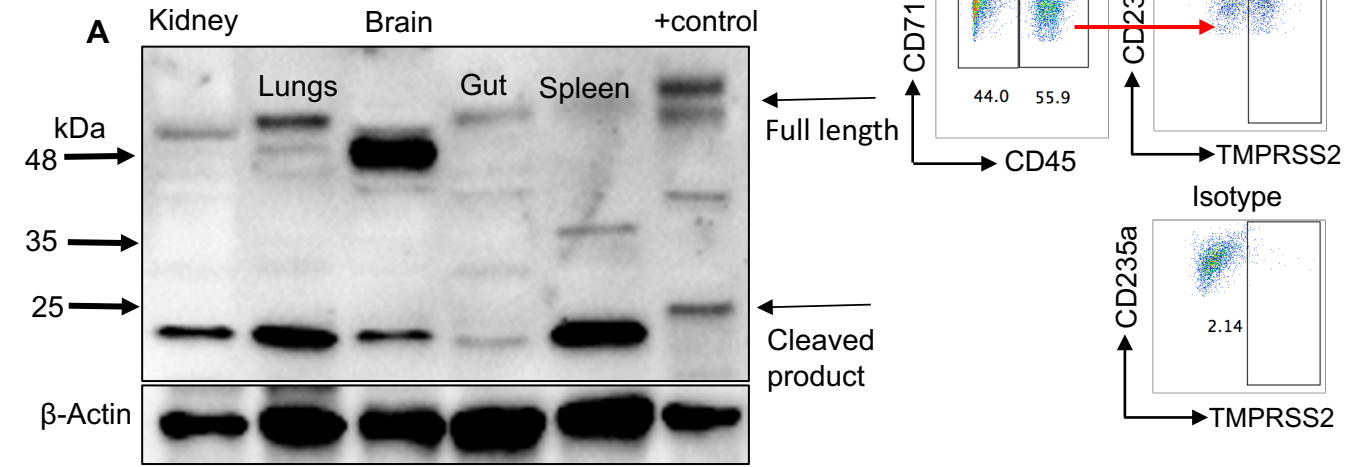


S. Fig. 4

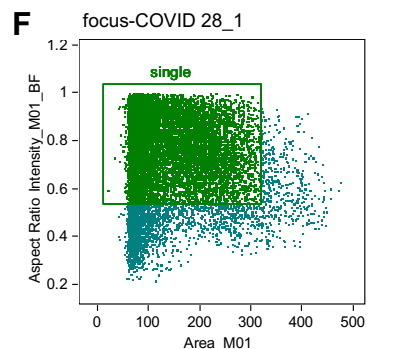




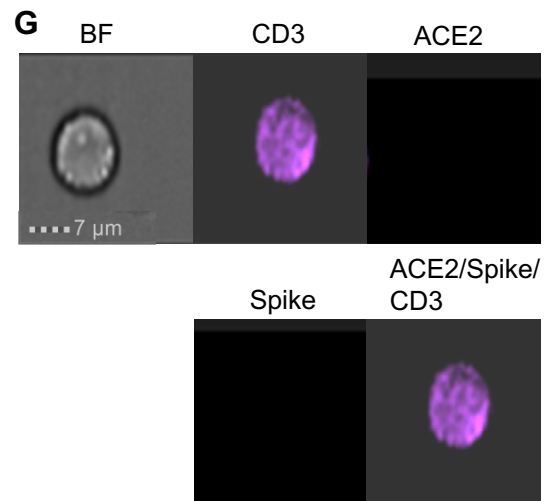
S. Fig. 5



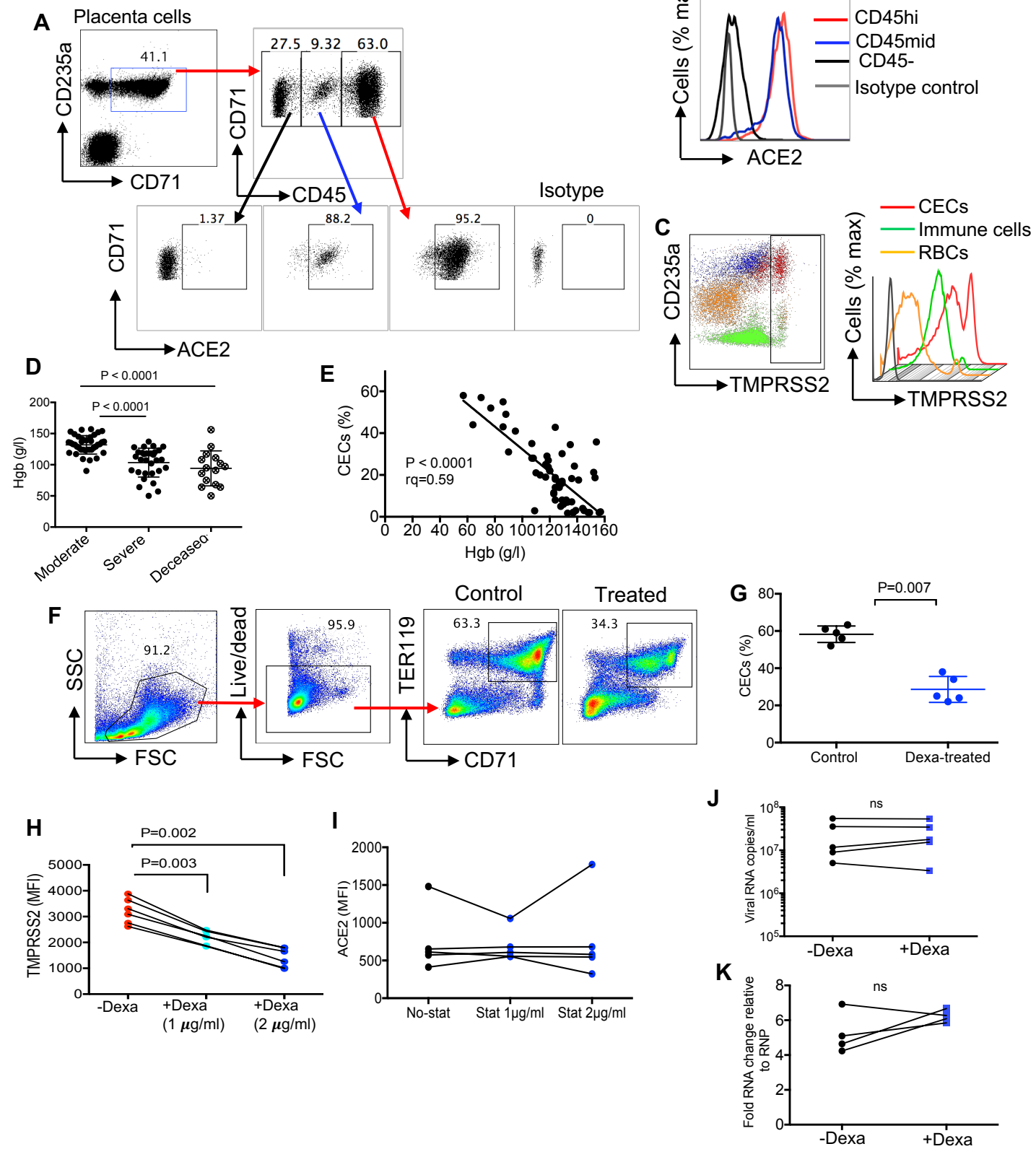
| Population              | Count | %Gated |
|-------------------------|-------|--------|
| single & focus          | 15461 | 100    |
| CD235a & single & focus | 3226  | 20.9   |



| Population     | Count | %Gated |
|----------------|-------|--------|
| focus          | 18374 | 100    |
| single & focus | 15461 | 84.1   |



S. Fig. 6



## Supplemental Figure Legends

**S Fig 1.** (A) Flow cytometry plots of gating strategy for CD71+CD235+ cells (CECs) in COVID-19 patients with severe and moderate disease. (B) Cumulative data of fold regulation for GATA-1 mRNA expression in CECs versus non-CECs (immune cell lineages) of > sex COVID-19 patients. (C) Cumulative data of fold regulation of ALAS2, HMBS, UROS, UROD, FECH, ALAD, PPOX and CPOX genes in CECs compared to non-CECs (immune cell lineages) of > six COVID-19 patients. (D) Representative plots, and (E) cumulative data showing the intensity of CD71 expression on total CECs versus immune cell lineages in PBMCs of COVID-19 patients. (F) Flow cytometry plots showing different subpopulation of CECs based on the expression of CD71, and (G) the intensity of CD71 expression as shown as by the geometric mean in each subpopulation (e.g. 1, 2, 3, 4 & 5) of CECs from PBMCs of a COVID-19 patient compared to immune cell lineages (Immune lin) and an isotype control. (H) Plots showing % of CD45+ cells within each subpopulation of CECs (e.g. 1, 2, 3, 4 & 5). (I) Representative flow cytometry plots, and (J) cumulative data of percentages of CD235a+CD71- cells in PBMCs of COVID-19 patients versus healthy controls (HCs). (K) Representative plot of the expression of PDL-1 and VISTA on CECs of a COVID-19 patient.

**S Fig 2.** (A) Representative histogram, and (B) cumulative data showing ROS expression in CECs compared to immune cell lineages of HIV-infected individuals. (C) Histogram of the purity of isolated CECs from PBMCs of a COVID-19 patient. (D) Cumulative data of CD107a in CD8 T cells following stimulation (Stim.) with SARS-CoV-2 peptides (2 µg/ml, 6 hr) without (W/out) or with (w) CECs (E) Gating strategy for plasma cells. (F) The correlation of % antibody secreting cells with % CECs in PBMCs of COVID-19 patients. (G) Image stream plots

showing the expression of ACE2 on CECs, and **(H)** the co-localization of ACE2 with CD71/CD235a or CD235a/ACE2 on CECs in PBMCs of COVID-19 patients.

**S. Fig 3.** **(A)** The presence of ACE2 in different organs/tissues of mice are shown by western blot. **(B)** Representative flow plot of the purity of isolated CECs from PBMCs of a COVID-19 patient used for western blot. **(C)** The comparison of ACE2 expression in VeroE6 cells (positive control) with immune cell lineages and CECs obtained from two different COVID-19 patients are shown by western blot. **(D)** Gating strategy for the identification of ACE2 expression on CECs, RBCs (CD235a+CD71-) and immune cell lineages (CD235a-CD71-). **(E)** Percentages of ACE2 expressing CECs among total CECs of a patient admitted to the ICU over time. **(F)** Representative, and **(G)** cumulative data showing intensity of CD147 on CECs versus RBCs (CD235a+CD71-) and other immune cell lineages as measured by the mean fluorescence intensity (MFI). **(H)** Representative plots of CD26/CD147 co-expression on CECs versus RBCs (CD235a+CD71- cells). **(I)** Histogram of the intensity of CD26 expression on CECs and RBCs versus isotype control in PBMCs of a COVID-19 patient. **(J)** Representative flow plots showing the expression of CD26 on CD45+CECs versus CD45-CECs in PBMCs of a COVID-19 patient.

**S Data Fig 4.** **(A)** Quantification of soluble ACE2 by ELISA in the plasma samples of COVID-19 patients compared to healthy controls (HCs). **(B)** Comparing soluble ACE2 levels in the plasma of COVID-19 patients at the time of hospital admission and 5-7 days later. **(C)** Longitudinal quantification of soluble ACE2 in the plasma of 3 patients at day 3 until 43 days post the admission to the ICU. **(D)** Gating strategy for the identification of TMPRSS2 expression on CECs, RBCs (CD235a+CD71-) and immune cell lineages. **(E, F)** Representative gating strategy for the identification of TMPRSS2 expressing CECs using Image stream analysis. **(G)** Image stream plots of TMPRSS2 expression on CECs from PBMCs of a COVID-19

patient. **(H)** Image stream plots of TMPRSS2 expression on CD14 monocytes in PBMCs of a COVID-19 patient.

**S Fig 5.** **(A)** The expression of TMPRSS2 in different organs/tissues of mice compared to the positive control (human colorectal adenocarcinoma grade II) are shown by western blot. **(B)** The expression of TMPRSS2 in CECs (CECs+) versus PBMCs-depleted of CECs (CECs-) from either COVID-19 patients or placental tissues (isolated CECs versus other cells (CECs-)) and cord blood compared to mouse lungs are shown by western blot. **(C)** Representative plots of TMPRSS2 surface expression on CD45+CECs of a human bone marrow. **(D)** Image stream plots of spike protein interaction/binding with ACE2 on CECs in PBMCs of a COVID-19 patient; bright field (BF) plus spike staining (BF + Spike), without spike staining (BF – Spike). **(E)** Gating strategy for the identification of CECs (CD235a+ cells) by the Image stream analyzer. **(F)** Representative plot is showing the area selection for CECs by the Image stream analyzer. **(G)** Image stream plots of spike protein interaction/binding with ACE2 on CECs T cells of a COVID-19 patient (BF + Spike) (the scale bar size for images is 7  $\mu$ m).

**S Fig 6.** **(A)** Flow plots showing the % expression of ACE2 on CD45-, CD45lo and CD45hiCECs of the placental tissue compared to the isotype control. **(B)** Histogram of the intensity of ACE2 expression on CD45-, CD45lo and CD45hiCECs of the placental tissue compared to the isotype control. **(C)** Plots showing the intensity of the expression of TMPRSS2 on total CECs compared to immune cells lineages and RBCs of the placental tissue. **(D)** Cumulative data showing the hemoglobin (Hgb) level in COVID-19 patients with moderate and severe disease versus those who deceased. **(E)** The correlation of Hgb levels with the proportion of CECs in the peripheral blood of COVID-19 patients. **(F)** Gating strategy and representative plots of CECs (CD71+TER119+) in mice. **(G)** Cumulative data of % CECs in control versus

treated mice with dexamethasone (1  $\mu\text{g/g}$  body weight) and quantified 2 days later. **(H)** Data of the expression of TMPRSS2 on CECs of COVID-19 patients once treated for 24 h without or with dexamethasone at 1 or 2  $\mu\text{g/ml}$ . **(I)** Data of ACE2 expression on CECs obtained from COVID-19 patients once treated for 24 h with or without atorvastatin (stat) at 1 or 2  $\mu\text{g/ml}$  as measured by mean fluorescence intensity (MFI). **(J)** Viral RNA copies in culture supernatants of monocytes either untreated or treated with dexamethasone (2  $\mu\text{g/ml}$ ) for 24 hr before infection with SARS-CoV-2 as measured 24 post-infection. **(K)** Cellular fold RNA changes relative to the housekeeping gene (RNP) in cell pellet of monocytes either untreated or treated with dexamethasone (2  $\mu\text{g/ml}$ ) for 24 hr before infection with SARS-CoV-2 as measured 24 hr post-infection.